

## Biquadratic Exchange Coupling in Sputtered (100) Fe/Cr/Fe

A. Azevedo, C. Chesman, S. M. Rezende, and F. M. de Aguiar

*Departamento de Física, Universidade Federal de Pernambuco, 50670-901 Recife-PE, Brazil*

X. Bian and S. S. P. Parkin

*IBM Research Division, Almaden Research Center, 650 Harry Road, San Jose, California 95120-6099*

(Received 12 January 1996)

We have used Brillouin light scattering, ferromagnetic resonance, magneto-optical Kerr effect, and magnetoresistance to investigate interlayer exchange coupling in Fe(40 Å)/Cr(*t*)/Fe(40 Å) trilayers grown onto MgO(100) in UHV. Unprecedented strong room-temperature biquadratic exchange coupling (BEC) was found for values of the Cr thickness *t* corresponding to a region where Fe layers are weakly antiferromagnetically coupled. A common feature in both magnetic and transport measurements, which we take as a signature of the BEC, is the presence of sudden discontinuous jumps as the external magnetic field is varied. The results are in excellent agreement with model calculations that coherently take into account the same phenomenological parameters characterizing the anisotropy, Zeeman, and bilinear and biquadratic exchange energies. [S0031-9007(96)00287-6]

PACS numbers: 75.70.Cn, 73.20.Dx, 75.30.Et, 78.35.+c

Lately magnetic exchange interactions between ferromagnetic films separated by nonmagnetic spacers have been widely investigated. The antiferromagnetic coupling [1], giant magnetoresistance [2], and oscillatory behavior of the exchange coupling [3] raised the expectations for exciting applications and new fundamental properties. The exchange coupling through nonmagnetic interlayers strongly depends on the thickness and nature of the spacer as well as on the interface roughness. This coupling is usually dominated by a Heisenberg type interaction bilinear in the films magnetizations. However, there is increasing evidence that near the transition from ferromagnetic to antiferromagnetic (AF) coupling a non-Heisenberg biquadratic term plays a remarkable role. This term is responsible for the peculiar effect of 90° alignment between the magnetizations of the ferromagnetic films, as recently observed in Fe/Cr/Fe (001) wedges [4,5], and trilayers of Co/Cu/Co (001) [6], Fe/Al/Fe (100) [7], and Fe/Ag/Fe [8]. Over the last few years several mechanisms have been proposed for the origin of the biquadratic exchange coupling (BEC) [9–12], which has recently been shown to be suppressed below the Néel temperature of Cr in the thick Cr regime in Fe/Cr superlattices [13]. In this work, we report a detailed experimental investigation of the BEC in sputtered Fe/Cr/Fe trilayers in the thin Cr regime at room temperature. We have also developed model calculations which correlate quite well the experimental results for a common set of phenomenological parameters, thus providing a unified picture of this effect in the Fe/Cr system.

Several samples of Fe(40 Å)/Cr(*t*)/Fe(40 Å) were grown by magnetron sputter deposition in a UHV chamber [14] onto polished, chemically cleaned single-crystal MgO(100) substrates, with  $5 < t < 35$  Å, a range that corresponds to the first two “antiferromagnetic peaks,” as shown in the upper inset of Fig. 1. Pronounced BEC was observed in samples at the right-hand side of the first AF

peak. The results presented henceforth were obtained in the sample with  $t = 15$  Å. Figure 1 shows the in-plane easy-axis magnetization curve obtained with the standard magneto-optical Kerr effect (MOKE) technique. One can clearly identify three distinct regions in this curve: In the low-field region (0–80 Oe), the linear response is a signature of the weak AF coupling between the two Fe films. The magnetization vectors of the two Fe films are nearly antiparallel in this region and small deviations from the antiparallel state might be induced by the external field *H*. Above 80 Oe, two hysteresis loops centered at  $H_1 \sim 100$  Oe and  $H_2 \sim 210$  Oe are

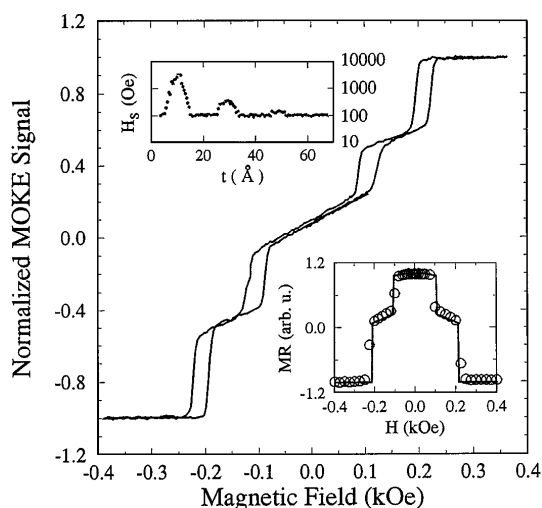


FIG. 1. Measured MOKE easy-axis hysteresis loop in the Fe(40 Å)/Cr(15 Å)/Fe(40 Å) sample. Upper inset: Measured saturation field in a Fe/Cr/Fe wedge as a function of the Cr thickness [14]. Lower inset: Open circles, measured room-temperature magnetoresistance in the same Fe(40 Å)/Cr(15 Å)/Fe(40 Å) of the main figure (peak MR is a 0.7% effect); the solid line is a fit with the expression  $1 - \cos(\phi_1 - \phi_2)$ .

observed. Intriguingly, the four-probe magnetoresistance measurement (only the down-field sweep is shown in the lower inset of Fig. 1) exhibits corresponding loops at the same field values. In order to explore even further this phenomenon, we also used the Brillouin light scattering (BLS) and the ferromagnetic resonance (FMR) techniques, as discussed below.

BLS measurements were carried out in the backscattering geometry, using a Sandercock tandem Fabry-Pérot (FP) interferometer in a  $(2 \times 3)$ -pass configuration. The light source was a single-mode-stabilized argon ion laser operating at  $5145 \text{ \AA}$  with incident power of 100 mW. The sample was mounted between the poles of an electromagnet with the field parallel to the incidence plane of the light beam and to an easy-magnetization axis. All the BLS spectra were measured at room temperature with an incident angle of  $30^\circ$ , corresponding to a scattering in-plane spin-wave wave number  $k \sim 1.22 \times 10^5 \text{ cm}^{-1}$ . The collimated light beam at the output of the FP interferometer was focused on a solid-state photodetector with 40% quantum efficiency at  $5145 \text{ \AA}$  and a dark count less than 2 counts/s, connected to a multichannel board in a computer. Surprisingly, we have been able to observe both so-called "acoustic" and "optical" modes in the field range of  $\pm 400 \text{ Oe}$ , within typically 10 to 15 min for each spectrum, the acoustic mode being more intense than the optical one. This allowed us to verify that for each region of the magnetization curve, there is a nicely corresponding spectrum of scattered light. In Fig. 2 we show four rep-

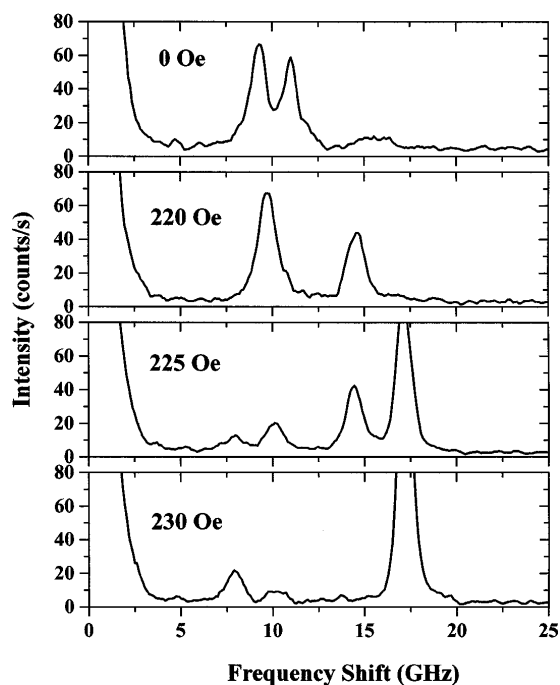


FIG. 2. Measured BLS spectra in  $\text{Fe}(40 \text{ \AA})/\text{Cr}(15 \text{ \AA})/\text{Fe}(40 \text{ \AA})$  for four different values of the applied field, corresponding to different regions of the magnetization curve shown in Fig. 1.

resentative spectra. In the low-field region, the modes are separated by approximately 2 GHz, the optical mode being at higher frequency [Fig. 2(a)]. For  $H_1 < H < H_2$ , and outside the hysteresis loops, there is an abrupt increase in this separation that reaches a value up to 7 GHz at higher fields [Fig. 2(b)]. Within a hysteresis loop, we have been able to observe four peaks at each side of the laser line [Fig. 2(c)], which shows unambiguously the bistable nature of this region. Finally, for  $H > H_2$ , the separation between the modes is again abruptly increased, this time being followed by an inversion of the modes positions with respect to the laser line. The measured up-field dispersion relation is shown by the solid (acoustic mode) and open (optical mode) circles in Fig. 3.

The FMR measurements were performed at 9.4 GHz by monitoring the derivative of the absorption line reflected from a  $\text{TE}_{102}$  rectangular microwave cavity with  $Q = 2500$ . A typical spectrum is shown in the inset of Fig. 4, which in turn shows the dependence of the in-plane resonance field as a function of the angular position with respect to  $H$ . The spectrum shown in the inset presents the FMR absorption lines for an angle  $\phi = 30^\circ$  with respect to the (easy)  $[100]$  direction. As in the BLS experiments, we were able to observe both the acoustic and optical modes. The linewidth of the acoustic mode,  $\Delta H \sim 25 \text{ Oe}$ , is comparable to the linewidth of molecular beam epitaxy-grown samples [15], which demonstrates that our sandwich is indeed single crystalline.

The overall behavior can be well described in terms of the free energy per unit area,

$$E = E_a + E_z + E_{ex}, \quad (1)$$

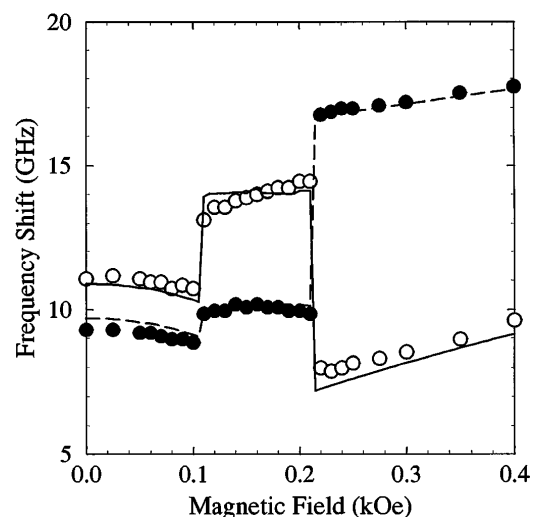


FIG. 3. BLS spin-wave dispersion relation observed in  $\text{Fe}(40 \text{ \AA})/\text{Cr}(15 \text{ \AA})/\text{Fe}(40 \text{ \AA})$ , showing the behavior of the acoustic (solid circles) and optical (open circles) modes as a function of the applied field. The corresponding dashed and solid lines are results of numerical simulations, as described in the text.

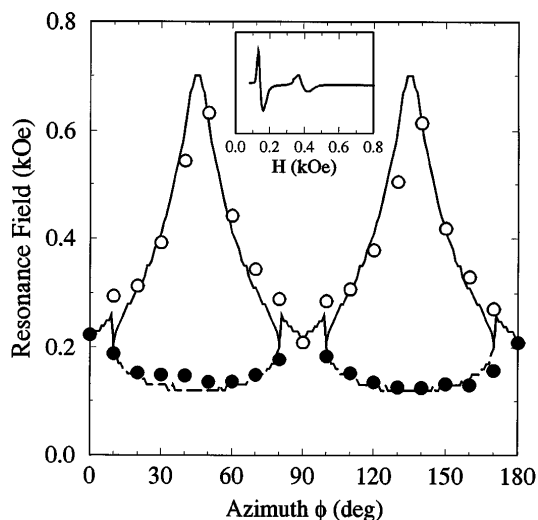


FIG. 4. Resonance fields at 9.4 GHz in Fe(40 Å)/Cr(15 Å)/Fe(40 Å), showing the behavior of the acoustic (solid circles) and optical (open circles) modes as a function of the azimuth angle  $\phi$  between an easy axis and the applied in-plane field. The corresponding dashed and solid lines are results of numerical simulations, as described in the text. Inset: FMR spectrum for  $\phi = 30^\circ$ .

where  $E_a$  is the anisotropy term,  $E_Z$  is the Zeeman energy, and  $E_{\text{ex}}$  is the exchange coupling energy. The latter can be written in the form

$$E_{\text{ex}} = -J_1 \hat{M}_1 \cdot \hat{M}_2 + J_2 (\hat{M}_1 \cdot \hat{M}_2)^2, \quad (2)$$

where  $J_1$  and  $J_2$  are the so-called bilinear and biquadratic coupling constants, and  $\hat{M}_1$  and  $\hat{M}_2$  are the unit magnetization vectors of the two ferromagnetic films. For dominant  $J_1$ ,  $\hat{M}_1$  and  $\hat{M}_2$  are ferromagnetically or antiferromagnetically coupled for  $J_1 > 0$  and  $J_1 < 0$ , respectively. However, if  $|J_2| > |J_1|$  and  $J_2 > 0$ , the magnetizations in the two films prefer to lie  $90^\circ$  to one another, in plane, in zero magnetic field.

In order to fit the MOKE data, the equilibrium positions of the magnetizations with respect to the in-plane field, namely,  $\phi_1$  and  $\phi_2$ , were numerically calculated from the minimum of the magnetic free energy given in Eq. (1). The inset of Fig. 5 shows the variation of  $\phi_1$  and  $\phi_2$  as a function of the field, exhibiting three phases: AF alignment occurs in the low-field region, a  $90^\circ$  coupling prevails in the mid-field range and the magnetizations are aligned with the field in the third region (saturation). Strikingly, the two transitions are of first order nature, in contrast to the pure AF (bilinear) coupling, where the transition between the spin-flop and saturated phases is of second order. The solid line in Fig. 5 is the sum  $(\cos\phi_1 + \cos\phi_2)/2$ , which presumably reflects the MOKE measurement (open circles), since only the components along the applied field are relevant.

The uniform and spin-wave modes that are measured by FMR and BLS are the eigenmodes calculated from

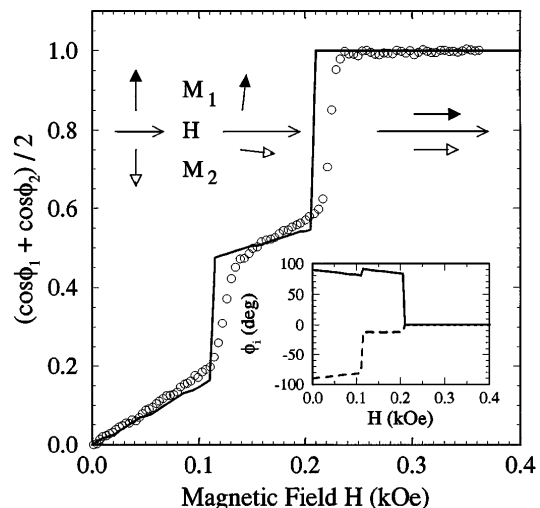


FIG. 5. Calculated magnetization curve (solid line), as described in the text. The open circles are the corresponding upfield MOKE measurements. Inset: Calculated equilibrium positions  $\phi_1$  (solid line) and  $\phi_2$  (dashed line).

the linearized Landau-Lifshitz equation of motion, assuming a small deviation of the magnetization vectors from their equilibrium positions [16]. The wave-vector dependence is introduced through the effective dipolar field [17]. A detailed account of the theoretical approach, including magnetoresistance calculations, will be published separately. Here we present results of the simultaneous numerical simulation of the MOKE (Fig. 5), MR (Fig. 1), BLS (Fig. 3), and FMR (Fig. 4) data for the following set of realistic parameters:  $4\pi M_s = 19.0$  kG ( $M_s$  is saturation magnetization),  $2K_1/M_s = 0.55$  kOe (anisotropy field),  $J_1/M_s t_{\text{Fe}} = -150$  Oe, and  $J_2/M_s t_{\text{Fe}} = 50$  Oe ( $t_{\text{Fe}}$  is Fe thickness). Since the dynamic response depends on the static configuration of the magnetizations, the excitation frequencies change abruptly at the two phase transitions, as seen in the BLS results. The overall agreement between the numerical results and the static and dynamical responses is quite impressive. Notice that long-range ordering of the Cr is not expected for  $t < 42$  Å [13]. Thus the results presented here might not change dramatically with temperature; i.e., no suppression of the BEC should be expected. Experiments which explore the dependence of the BEC on  $t_{\text{Fe}}$  will be carried out shortly. This should give some insight on the microscopic nature of the coupling in the Fe/Cr system.

In summary, we have performed magnetic and transport measurements to investigate the exchange coupling interaction between the two Fe films in Fe/Cr/Fe sandwiches. For a Cr thickness of 15 Å, it is clearly demonstrated that the bilinear exchange AF coupling is relatively weak and that an unrivaled strong room-temperature BEC plays a remarkable role. To our knowledge, a coherent fit of the data from various experimental techniques with the same

set of phenomenological parameters is provided for the first time.

We would like to thank K. P. Roche for technical support and M. Lucena for helping in some measurements. The work at UFPE has been supported by CNPq, CAPES, PADCT, FINEP, and FACEPE (Brazilian agencies). The work at IBM was partially supported by the Office of Naval Research. X. Bian acknowledges a postdoctoral fellowship from the Natural Sciences and Engineering Research Council of Canada.

- 
- [1] P. Grünberg, R. Schreiber, Y. Pang, M. O. Brodsky, and H. Sowers, *Phys. Rev. Lett.* **57**, 2442 (1986).
  - [2] M. N. Baibich, J. M. Broto, A. Fert, F. Nguyen Van Dau, F. Petroff, P. Etienne, G. Creuzet, A. Friederich, and J. Chazelas, *Phys. Rev. Lett.* **61**, 2472 (1988).
  - [3] S. S. P. Parkin, N. More, and K. P. Roche, *Phys. Rev. Lett.* **64**, 2304 (1990).
  - [4] M. Ruhrig, R. Schafer, A. Hubert, R. Mosler, J. A. Wolf, S. Demokritov, and P. Grünberg, *Phys. Status Solidi A* **125**, 635 (1991).
  - [5] J. Unguris, R. J. Celotta, and D. T. Pierce, *Phys. Rev. Lett.* **67**, 140 (1991).
  - [6] B. Heinrich, J. F. Cochran, M. Kowalewski, J. Kirschner, Z. Celinski, A. S. Arrot, and K. Myrtle, *Phys. Rev. B* **44**, 9348 (1991).
  - [7] M. E. Filipkowski, C. J. Gutierrez, J. J. Krebs, and G. A. Prinz, *J. Appl. Phys.* **73**, 5963 (1993).
  - [8] Z. Celinski, B. Heinrich, and J. F. Cochran, *J. Appl. Phys.* **73**, 5966 (1993).
  - [9] J. Slonczewski, *Phys. Rev. Lett.* **67**, 3172 (1991).
  - [10] J. Barnas and P. Grünberg, *J. Magn. Magn. Mater.* **126**, 380 (1993).
  - [11] R. P. Erickson, K. B. Hathaway, and J. R. Cullen, *Phys. Rev. B* **47**, 2626 (1993).
  - [12] D. M. Edwards, J. M. Ward, and J. Mathon, *J. Magn. Magn. Mater.* **126**, 380 (1993).
  - [13] E. C. Fullerton *et al.*, *Phys. Rev. Lett.* **75**, 330 (1995).
  - [14] X. Bian, H. T. Hardner, and S. S. P. Parkin, in *Proceedings of the MMM 95* (to be published).
  - [15] J. J. Krebs, P. Lubitz, A. Chaiken, and G. A. Prinz, *Phys. Rev. Lett.* **63**, 1645 (1989).
  - [16] J. F. Cochran *et al.*, *Phys. Rev. B* **42**, 508 (1990).
  - [17] R. L. Stamps, *Phys. Rev. B* **49**, 339 (1994).